Received: 11 June 2020 | Revised: 13 January 2021 | Accepted: 14 January 2021

DOI: 10.1111/mec.15813

ORIGINAL ARTICLE

MOLECULAR ECOLOGY WILEY

Genomic signatures of selection in bats surviving white-nose syndrome

Sarah A. Gignoux-Wolfsohn[1] | Malin L. Pinsky[1] | Kathleen Kerwin[1] | Carl Herzog[2] | MacKenzie Hall[3] | Alyssa B. Bennett[4] | Nina H. Fefferman[5,6] | Brooke Maslo[1]

[1]Department of Ecology, Evolution, and Natural Resources, Rutgers, The State University of New Jersey, New Brunswick, NJ, USA

[2]New York State Department of Environmental Conservation, Albany, NY, USA

[3]Endangered and Nongame Species Program, New Jersey Department of Environmental Protection, Trenton, NJ, USA

[4]Vermont Fish and Wildlife Department, Rutland, VT, USA

[5]Ecology and Evolutionary Biology, University of Tennessee, Knoxville, TN, USA

[6]National Institute for Mathematical and Biological Synthesis, University of Tennessee, TN, USA

Correspondence
Sarah A. Gignoux-Wolfsohn, Smithsonian Environmental Research Center, Edgewater, MD, USA.
Email: gw.sarah@gmail.com

Funding information
US National Science Foundation, Grant/Award Number: #OCE-1426891; United States Fish and Wildlife Service, Grant/Award Number: F15AP00949

Abstract

Rapid evolution of advantageous traits following abrupt environmental change can help populations recover from demographic decline. However, for many introduced diseases affecting longer-lived, slower reproducing hosts, mortality is likely to outpace the acquisition of adaptive de novo mutations. Adaptive alleles must therefore be selected from standing genetic variation, a process that leaves few detectable genomic signatures. Here, we present whole genome evidence for selection in bat populations that are recovering from white-nose syndrome (WNS). We collected samples both during and after a WNS-induced mass mortality event in two little brown bat populations that are beginning to show signs of recovery and found signatures of soft sweeps from standing genetic variation at multiple loci throughout the genome. We identified one locus putatively under selection in a gene associated with the immune system. Multiple loci putatively under selection were located within genes previously linked to host response to WNS as well as to changes in metabolism during hibernation. Results from two additional populations suggested that loci under selection may differ somewhat among populations. Through these findings, we suggest that WNS-induced selection may contribute to genetic resistance in this slowly reproducing species threatened with extinction.

KEYWORDS
disease-induced selection, evolutionary rescue, *Myotis lucifugus*, white-nose syndrome

1 | INTRODUCTION

Organisms can evolve in response to abrupt environmental change (Conover et al., 2006; Darimont et al., 2009; Thompson, 1998), including the introduction of novel pathogens (Epstein et al., 2016). However, when host populations are long-lived and introduced pathogens cause mass mortalities, rapid evolution is unlikely to occur through de novo mutation. Recently, selection through soft sweeps has been proposed as a common and possibly dominant method of selection that has been largely overlooked (Messer & Petrov, 2013). Soft sweeps from standing genetic variation may be a common mechanism of disease-induced selection, but compared to hard sweeps, which result in high linkage disequilibrium and a clear reduction in diversity surrounding the area under selection, soft sweeps leave few detectable signatures in genomes sampled after the mass mortality event has ended (Messer & Petrov, 2013; Przeworski et al., 2005). Our understanding of disease-induced evolution and its role in population recovery in long-lived organisms therefore remains limited. Using samples collected over time, recent studies have identified signatures of pathogen-induced selection in taxa such as bees (Mikheyev et al., 2015), sea stars (Schiebelhut et al., 2018), Tasmanian devils (Epstein et al., 2016) and bats (Auteri & Knowles, 2020). As globalization and climate change increase the

number and frequency of epizootics across all taxa (Burge et al., 2014), the ability to identify rapid evolution from standing genetic variation in recovering and persisting populations will be crucial to understanding the impacts of novel pathogens.

Some of the most dramatic disease-induced mass mortality events in recent years are the declines of North American bat species due to white-nose syndrome (WNS), an infectious disease caused by the introduced fungal pathogen *Pseudogymnoascus destructans* (Frick, Pollock, et al., 2010; Gargas et al., 2009). *P. destructans* infects bats during hibernation; it creates lesions in wing membranes, disrupts homeostasis and depletes energy stores by altering metabolism and increasing the frequency of arousal from torpor (Gargas et al., 2009; Reeder et al., 2012). The previously widespread little brown bat (*Myotis lucifugus*) is one of the most heavily impacted species (Kunz & Reichard, 2010). The effects of WNS on *M. lucifugus* population abundance vary widely, with some hibernating colonies having undergone apparent extirpation (Frick et al., 2015, 2017), others experiencing continued and persistent declines, and still others returning to neutral or positive growth after declines of up to 98% (Frick et al., 2017; Maslo & Fefferman, 2015; Vander Wal et al., 2013). Analyses of population declines and infection rates suggest that host resistance is a more likely mechanism behind observed positive population trajectories, rather than alternative mechanisms such as host tolerance, demographic compensation or reduced pathogen virulence (Langwig et al., 2017), although debate on this point continues.

A recent study identified signatures of selection in *M. lucifugus* by comparing WNS survivors and nonsurvivors from across Michigan, USA, where populations are continuing to decline, suggesting that WNS can select for alleles related to hibernation behaviour, metabolism and vocalization (Auteri & Knowles, 2020). Despite the hypothesis that immune-related genes are probable targets of WNS-related selection (Donaldson et al., 2017), immune-related genes were not apparent targets of selection in Michigan (Auteri & Knowles, 2020), a result compatible with survivor allele frequency differences between New York and Pennsylvania (Lilley et al., 2020). Whether targets of selection are consistent across different geographical regions remains unclear, however. In addition, the broad geographical range achieved through opportunistic sampling (Auteri & Knowles, 2020; Lilley et al., 2020) makes it difficult to eliminate the potentially confounding effects of geographical variation in allele frequencies. Ideally, signatures of selection can best be identified by comparing samples taken from the same populations through time. Tracking changes in allele frequencies of populations with known trajectories is an important step to understanding whether evolutionary changes may help these populations avoid extinction and persist through evolutionary rescue (Vander Wal et al., 2013).

Here, we performed whole genome sequencing on *M. lucifugus* nonsurvivors collected from the first group of WNS-induced mass mortalities and survivors sampled several years later from four hibernating colonies (hibernacula) within the epicentre of WNS emergence. We first looked at structure between hibernacula as well as between survivors and nonsurvivors (i.e., genome-wide differences between time points). Then, using paired samples of survivors and nonsurvivors from each of two hibernacula that are currently in the early stages of recovery, we were able to test for (i) genetic signatures of population bottlenecks and (ii) signatures of WNS-induced selection in both populations that may be associated with survival. We found signatures of soft selective sweeps from standing genetic variation in several genes associated with the immune system, hibernation and metabolism.

2 | MATERIALS AND METHODS

2.1 | Study area

Hibernacula in the northeastern United States were the first to be affected by WNS in North America. Individual dead (nonsurvivor) bats were collected and frozen when WNS mortalities were first

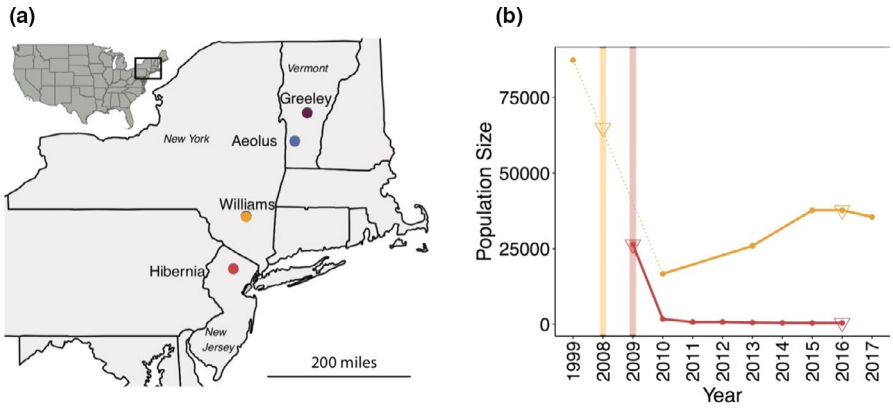

FIGURE 1 Four hibernacula were sampled across time and are experiencing different rates of population recovery. (a) Location of hibernacula sampled in the northeast United States. (b) Population trajectories for Williams and Hibernia, colour coded according to (a). Vertical lines represent the time of initial reports of white-nose syndrome (WNS) for each hibernaculum. The dotted line represents missing data for Williams because population estimates were not made between 1999 and 2010 (1999 is the presumed pre-WNS baseline). The triangles indicate sampling points for each hibernaculum. Population estimates were not available for Greeley and Aeolus

observed at Walter Williams Preserve (Williams), Ulster County, New York (2008, *n* = 30); Hibernia Mine (Hibernia), Morris County, New Jersey (2009, *n* = 26); and Greeley Mine (Greeley), Windsor County, Vermont (2009, *n* = 30; Figure 1a). All three hibernacula are abandoned mines, with Williams the largest in size. These individuals provided us with samples from nonsurvivors. Sample collection followed Simmons (2009). Briefly, a 2-mm wing tissue biopsy was taken (Miltex) and placed in RNALater (Ambion). Because large proportions of both populations died during the initial WNS outbreak, these bats are representative of the genetic diversity from before the introduction of WNS. However, because these samples are specifically from nonsurvivors, they may be enriched for alleles that makes bats more susceptible to WNS.

In 2016 (one to two generations later), we returned to collect samples from living survivors of WNS from Williams (*n* = 30) and Hibernia (*n* = 30). Because Greeley Mine was inaccessible at that time, samples were instead taken from Aeolus Cave (Aeolus), Bennington County, Vermont (*n* = 30), which was the only accessible hibernaculum in Vermont, but was 66 km away. We therefore did not include Greeley or Aeolus in any calculations of change in allele frequencies. These survivors were sampled by taking a wing punch from live hibernating adults (>1 year old) within the remnant population. Age cannot be determined beyond this as bats do not show outward signs of senescence, become reproductive after 1 year and can live up to 40 years, with most adults maintaining their reproductive status (Frick et al., 2010; Keen & Hitchcock, 1980). Therefore, individuals sampled post-WNS were either survivors of the initial mass mortality or were born from survivors of the mass mortalities. Samples were collected under IACUC Protocol #15-068 (Rutgers University) and appropriate state permits.

2.2 | Population sizes and growth rate

Population census counts of hibernating bats were conducted during winter months at Williams and Hibernia. The first count at Williams was conducted a year after the first mortality and can be compared to a generally accepted pre-WNS population size from 1999 (C. Herzog, New York State Department of Environmental Conservation, unpublished data). The first count conducted at Hibernia coincided with the first discovery of WNS-induced mortality at this site and is therefore not likely to be representative of pre-WNS population size. At Hibernia, population monitoring activities were carried out by B. Maslo under the authority of a cooperative agreement between the New Jersey Division of Fish and Wildlife (formerly NJ Division of Fish, Game and Shellfisheries) and the US Fish and Wildlife Service dated June 23, 1976. National White-nose Syndrome Decontamination Protocols ("National White-nose Syndrome Decontamination Protocols") were followed during all visits. Population sizes for Greeley and Aeolus were not available.

In addition, we used mark–recapture methods at Hibernia to measure survival and calculate population growth rates and changes through time. During annual surveys from 2010 to 2017, we captured and marked 1262 (476 females, 786 males) little brown bats with unique 2.9-mm or 2.4-mm lipped alloy bands (Porzana Ltd). We analysed encounter histories of individuals using Cormack–Jolly–Seber (CJS) models in Program mark (White & Burnham, 1999) and examined the effects of sex, year and time since WNS arrival on annual survival. We developed 24 a priori candidate models containing combinations of constant, yearly, time trend and sex-specific effects on annual survival and recapture probabilities, including a global model that included time-dependent and sex-specific survival and recapture. To test for goodness of fit, we used a parametric bootstrapping procedure with 500 simulations of our penultimate model and calculated a variance inflation factor of $\hat{c}$ = 1.26. Because we detected slight overdispersion in our data, we used small-sample-corrected Quasi-Akaike's Information Criterion ($QAIC_C$) adjusted by $\hat{c}$ = 1.26 (Burnham & Anderson, 2002). We ranked candidate models by $\Delta QAIC_C$ and Quasi-Akaike weights (*w*), which represent the relative likelihood of the model given the data (Johnson & Omland, 2004). To reduce model selection bias and uncertainty, we averaged all models contributing to cumulative $w \geq 0.85$ (top five models) and calculated parameter estimates based on weighted averages of the parameter estimates in the top models (Burnham & Anderson, 2002; Burnham et al., 2011). Model results confirmed previously published findings (Maslo et al., 2015) of a linear increase in annual survival with time since WNS arrival. Recapture rates averaged ~0.40 for both sexes.

To determine the post-WNS growth rate of the remnant Hibernia population, we incorporated our survival estimates into seven two-stage Lefkovitch matrices (*35–37*). Each matrix represented one study year from 2010 to 2016:

$$\begin{bmatrix} S_j * B_j * Fe & S_a * B_a * Fe \\ S_j & S_a \end{bmatrix}$$

where *S* represents survival of female little brown bats; *B* represents the probability that a female breeds; and subscripts *j* and *a* indicate values for juveniles or adults, respectively. Little brown bats have a single pup each year and are sexually mature by the end of their first summer, so we held fecundity (*Fe*) constant for both age classes at *Fe =1*. We assigned probability of breeding for adults and juveniles to values of *Bj =0.38* and *Ba =0.85*, respectively, based upon published estimates generated from either 15 years of pre-WNS mark–recapture data or post-WNS adult reproductive rates (Frick, Pollock, et al., 2010; Frick, Reynolds, et al., 2010; Reichard & Kunz, 2009). We fixed juvenile survival as a constant proportion of adult survival ($Sj = 0.47 \times S_a$; Frick, Pollock, et al., 2010). We then calculated the dominant eigenvalue of each matrix. We projected the Hibernia population through the 2010–2016 matrices and then continued the projection an additional 93 years using the 2016 matrix. We ran a 10,000-iteration Monte Carlo simulation, allowing S_a and B_j to vary stochastically based on random number generation from beta distributions specified from the means and variances of each survival parameter. From this procedure, we generated a mean stochastic yearly growth rate.

2.3 | Library preparation and sequencing

DNA was extracted using the QIAGEN Blood and Tissue kit with the addition of RNase A to remove RNA contamination and following recommendations to increase the concentration of DNA (10-min elution step, smaller volume of elution buffer). DNA was visualized using 1.5% gel electrophoresis and when fragments <1 kbp were present, a cleanup step was performed with AMPure XP beads (Agencourt). DNA concentration was measured using a Qubit HS DNA Assay (Invitrogen). Samples with concentrations below 1 ng/μl were not used for library preparation.

Libraries were prepared using the Illumina Nextera kit following the low-coverage whole genome sequencing protocol developed by Therkildsen and Palumbi (2016), modified from Baym *et al.* (2015). Briefly, samples were fragmented and adapters were added using tagmentase in a 2.5-μl volume. The ideal concentration of DNA to achieve appropriately sized fragments given the size of the *Myotis lucifugus* genome was determined to be 10 ng/μl. However, 10 ng/μl was above the concentration for many of our samples, so we diluted the tagmentase for low-concentration samples using 10× TB in order to achieve the same ratio of tagmentase to DNA and therefore equal fragment length.

A two-step PCR (polymerase chain reaction) procedure was then conducted: first eight cycles using the KAPA Library Amplification kit and the Nextera index kit (primers N517-N504 and N701-N706) to add a unique combination of barcodes to each sample followed by four cycles to amplify the resulting libraries using "reconditioning" primers found in Therkildsen and Palumbi (2016). We purified and size selected these products with AMPure XP beads, quantified the concentration of each library using a Qubit HS DNA Assay, and examined the fragment size using an Agilent BioAnalyzer chip. Finally, we pooled the resulting libraries together in equal concentrations by mass. These pools were sequenced in seven rapid runs (each with two lanes per run) on the Illumina HiSeq 2500 at the Princeton University Lewis-Siegler Institute. We achieved an average depth of coverage per population (a particular geographical site at a particular time point) of 52.55 ± 9.03 (Table S1). This depth of coverage allowed us to identify single nucleotide polymorphisms (SNPs) and calculate population-level allele frequencies using established methods that take genotype uncertainty into account (Korneliussen et al., 2014; Nielsen et al., 2012). We did not need nor attempt to call individual genotypes. Probabilistic approaches such as those used here have increased efficiency, precision and cost-effectiveness for estimating allele frequencies as compared to calling individual genotypes (Alex Buerkle & Gompert, 2013; Therkildsen & Palumbi, 2016), which can place undue confidence in genotype calls and skew population-level allele frequency estimates. Furthermore, by distinguishing between individuals and accounting for differences in read depth, our approach eliminates nonequimolar DNA errors or stochastic amplification differences associated with Pool-seq approaches (Anderson et al., 2014; Cutler & Jensen, 2010; Therkildsen & Palumbi, 2016).

2.4 | Code availability

All scripts and notebooks can be found at https://github.com/sagw/WNS_WGS/ and relative paths referenced below are to be appended to this base path.

2.5 | Bioinformatics

To remove exact duplicate sequences (probably optical duplicates), we ran FASTUNIQ in paired-end mode. We then used trimmomatic version 0.36 in paired-end mode to remove Illumina adapters, remove reads with an average Phred score below 33, trim any reads where a 4-bp sliding window Phred score fell below 15, and discard trimmed reads shorter than 30 bp.

We flagged contaminant sequences using FASTQSCREEN version 0.95 (https://www.bioinformatics.babraham.ac.uk/projects/fastq_screen/) with BOWTIE2. Reads were screened against the human genome (ch38), all bacterial genomes, all fungal genomes including *Pseudogymnoascus destructans*, and all viral genomes available from NCBI (ftp://ftp.ncbi.nlm.nih.gov/genomes/genbank/). Unpaired reads were removed using FASTQSCREEN in filter mode and from paired reads using a python script (Scripts/pfilter.py) to remove both reads in a pair. Less than 10% of reads were removed.

We mapped resulting paired and unpaired reads to the 2.035-Gbp *Myotis lucifugus* 2.0 genome (ftp://ftp.ensembl.org/pub/release-87/fasta/myotis_lucifugus/dna/, genome information available here: https://uswest.ensembl.org/Myotis_lucifugus/Info/Annotation) using BOWTIE2 in very sensitive local mode (Langmead & Salzberg, 2012). The genome has an N50 size of 4.3 Mbp. We then sorted SAM files, converted to BAM, and removed duplicate sequences using PICARD (https://broadinstitute.github.io/picard/) (MarkDuplicates). We used BEDTOOLS (Quinlan & Hall, 2010) to calculate percentage coverage and discarded individuals with reads that covered <20% of the genome. We used GEM (Derrien et al., 2012) to determine mapability of the reference genome. Only regions with a mapability score of 1 were used (1.7 out of 2.2 Gb). Finally, we removed repeat regions as determined using REPEATMASKER (Smit et al., 2013–2015).

2.6 | SNP calling and summary statistics

Following previous studies using low-coverage data (e.g., Mikheyev et al., 2015; Oziolor et al., 2019; Prince et al., 2017), we called SNPs over the 132 remaining samples (Table S1) using ANGSD (version 0.92) with the following parameters: the samtools model was used to estimate genotype likelihoods from the mapped reads (-GL 1) and major and minor alleles and frequency were estimated from genotype likelihoods (-doMaf 1 -doMajorMinor 1). We used the following quality filters (requires -doCounts 1): minimum quality score of 20, minimum mapping score of 30, minimum number of individuals with data of 68 (half the number of individuals), and maximum depth over all

individuals of 1320 (number of individuals ×100). SNPs were called by performing a likelihood ratio test of minor allele frequencies using a chi-square distribution and keeping loci with a *p*-value less than 10^{-6}. See Notebooks/Angsd_all_SNPs for code.

We calculated genotype likelihoods for identified SNPs with ANGSD in beagle format (-doGlf 2). These likelihoods were used with PCANGSD to (i) calculate a covariance matrix, (ii) determine the number of significant principal components (*D*) using Shriner's implementation of Velicer's minimum average partial (MAP) test, and (iii) determine admixture proportions using non-negative matrix factorization with the number of ancestral populations (*K*) calculated as *D* + 1 (Meisner & Albrechtsen, 2018). The principal components analysis (PCA) and admixture proportions were then visualized using R (see Notebooks/Angsd_all_SNPs and Notebooks/Angsd_all_PCA_graphs for code). We further used genotype likelihoods to estimate relatedness between all individuals using the IBS method of IBSRELATE (Waples et al., 2019).

In order to calculate F_{ST} between subpopulations, we first calculated unfolded sample allele frequencies with ANGSD using the reference genome to polarize the alleles for each subpopulation (-doSaf 1). We then created the following joint site frequency spectra with the ANGSD program REALSFS: Hibernia nonsurvivor:survivor, Williams nonsurvivor:survivor, Hibernia:Williams:Greeley nonsurvivor, Hibernia:Williams:Aeolus survivor. An average F_{ST} was calculated across the entire genome and in a sliding window across the genome. See Notebooks/Angsd_all_FST for code.

We then used the per-population sample allele frequencies to create unfolded site frequency spectra for each population. The sample allele frequencies and site frequency spectra were used to calculate θ (population mutation rate) across the genome (-doThetas 1), and then calculate θ_w, π and Tajima's *D* both across the genome and in a sliding window with the ANGSD program THETASTAT (do_stat -win 1000 -step 1 -type 1). See Notebooks/Angsd_all_thetas for code.

We estimated minor allele frequencies for each called SNP in each subpopulation using the previously inferred major and minor alleles (–doMajorMinor 3) and the same quality filters used when calling SNPs. To exclude regions that were over-sequenced and may therefore introduce bias, maximum depth was set at 270 (maximum number of individuals per population ×10). Allele frequency was summed over up to three possible minor alleles weighted by probabilities (–doMaf 2). To confirm that the stringent quality filters did not filter out divergent alleles, we also calculated allele frequencies with relaxed filters: minimum quality score of 5, minimum mapping score of 15 (Figure S1).

See Notebooks/Angsd_all_SNPs.

2.7 | Identifying SNPs putatively under selection

For the Hibernia and Williams colonies (Figure 1), a change in minor allele frequency was calculated from minor allele frequencies (MAFs, method 2) as $maf_{survivors} - maf_{nonsurvivors}$. Our method for testing for selection was computationally intensive, so we focused on loci with the strongest evidence for selection and only examined SNPs with a large change in allele frequency (absolute changes greater than 0.5) in the same direction in both Hibernia and Williams. Unless otherwise noted, all reported allele frequencies for this analysis are of the allele that was lowest in the nonsurvivors from Hibernia and Williams, making all changes in allele frequency positive.

Because large temporal changes in allele frequency can be caused by sampling error or genetic drift, we developed locus-specific null models for allele frequency change. We first accounted for sampling error by bootstrapping across the individuals in each sample and recalculating allele frequencies from each bootstrap for each SNP. We used ANGSD to calculate minor allele frequencies from 100 bootstrapped lists of individuals for Hibernia nonsurvivors and survivors and for Williams nonsurvivors and survivors. We estimated the generation time of *M. lucifugus* as 6 years, meaning more than one generation has elapsed between sample collection. To make our test more conservative, we used Wright–Fisher simulations to estimate genetic drift over two generations (Fisher, 1922; Wright, 1930). We initialized each Wright–Fisher simulation with one of the bootstrapped nonsurvivor allele frequencies and then ran the simulations forward using binomial sampling of alleles to produce simulated final allele frequencies. We did not attempt to correct for bias due to only sampling nonsurvivors. We then compared the final simulated allele frequency to a randomly selected estimate of the survivor allele frequency from the bootstrapped values. In this way, we accounted for sampling error by bootstrapping over individuals and for genetic drift by using the Wright–Fisher simulations. *p*-values were calculated for each SNP as $p = (r + 1)/(n + 1)$, where *r* was the number of times the simulated survivor allele frequencies were greater than sampled bootstrapped survivor allele frequencies, and *n* was the total number of simulations (North et al., 2002).

We estimated effective population size for the Wright–Fisher simulations from the Hibernia census data. We used known demographic information to calculate a ratio of effective to census population size (Waples et al., 2013), where average lifespan is 12 years, age to maturity is 1 year and generation time is 6 years (Frick, Reynolds, et al., 2010). The two generations in Hibernia have estimated effective population sizes of 424 and 296, respectively. Due to the smaller population size of Hibernia as compared to Williams, we probably overestimated drift in Williams, which had the effect of making our test more conservative. All code can be found in Notebooks/All_AlleleFreqChange.ipynb.

Because there is no evidence of substantial bat migration between colonies in the time frame of this study (even if populations were panmictic in evolutionary time), the Hibernia and Williams populations were considered independent. We therefore combined the *p*-values from each population using the sum log method in the R package METAP (*59*). To account for multiple hypothesis testing, *p*-values were then adjusted using the Benjamini–Hochberg method. Values were ranked from smallest to largest and the largest *p*-value with $p < (i/m)Q$ was used as the significance cut off, where *i* was rank,

m was the number of SNPs in both Hibernia and Williams, and *Q* was our chosen false discovery rate of 0.2. We show alternative rates in Figure S2.

We also tested whether the number of loci with large allele frequency changes shared across populations was larger than expected by chance. We calculated the number of shared SNPs expected to have an absolute allele frequency change >0.5 as a binomial sample where the probability of success was (proportion >0.5 in population 1) × (proportion >0.5 in population 2) and the number of trials was the total number of SNPs genotyped in both populations. In our case, these numbers were 0.00099 and 0.0011 for 40,952,833 loci genotyped. We sampled 10,000 times from the binomial distribution and report the median, 2.5th percentile and the 97.5th percentile.

2.8 | Putative SNPs of small effect

While the above analysis could successfully identify SNPs with large changes in allele frequency, we recognized that there could be a combination of SNPs with large and small effects on disease resistance. We therefore used a Cochran–Mantel–Haenszel (CMH) test adapted to account for genetic drift to identify additional SNPs, as implemented in the R package ACER (Spitzer et al., 2020). The CMH test allows for joint identification of multiple genetic variants associated with a categorical trait (here, survivor/nonsurvivor) across multiple populations.

2.9 | Estimating selection coefficients

For loci identified as candidate targets of selection, we next calculated the selection coefficient (*s*) consistent with a given change in allele frequency in a rejection-based Approximate Bayesian Computation (ABC) framework (Beaumont et al., 2002; Csillery et al., 2010). We ran forward Wright–Fisher simulations similar to those described above. We used the minor alleles as inferred by ANGSD, therefore allowing change in allele frequency to be either positive or negative. We sampled *s* values from a uniform prior (−1 to 1) so that selection could drive allele frequencies in either direction. Rather than a neutral probability, the probability of selecting the focal allele in the next generation (*x*) was calculated as

$$x = \frac{(1+s)p^2 + \left(1+\frac{s}{2}\right)p(1-p)}{(1+s)p^2 + 2\left(1+\frac{s}{2}\right)p(1-p) + (1-p)^2}$$

for frequency *p* in the previous generation. We assigned a score to each simulated survivor allele frequency based on its similarity to the bootstrapped survivor allele frequencies (higher scores indicated more similarity). Scores were calculated by comparing all simulated frequencies to all bootstrapped frequencies and increasing the score by 1 for the top 1000 simulated frequencies closest to a given bootstrapped frequency. To obtain the posterior distribution of *s*, we then sampled 100 *s* values weighted by this score. For each SNP, we calculated the mean, 2.5% and 97.5% quantiles of the posterior distribution. These simulations therefore accounted for sampling error, drift and selection. All code can be found in Notebooks/ Wfs_SCalculations.ipynb.

2.10 | Immigration

To estimate the likelihood that the observed changes in allele frequency were due to immigration between hibernacula rather than selection, we calculated immigration rates required to achieve these frequencies and compared them to known reports of immigration. The minimum detectable immigration rate that would be required to achieve the observed allele frequency changes was calculated as

$$P_{i0} = 100\left(\frac{F_{s1} - F_{ns1}}{F_{s2} - F_{ns1}}\right)$$

where P_{i0} is the percentahe of detectable (banded) immigrants in population 1 survivors, F_{s1} is the allele frequency in population 1 survivors, F_{ns1} is the allele frequency in population 1 nonsurvivors and F_{s2} is the allele frequency in population 2 survivors. If *t* generations have passed, the observed allele frequencies can be achieved with the minimum number of detectable immigrants when all immigration occurs at time 0. Assuming that with each successive generation the number of detectable immigrants stays the same, but half the number of residents and banded immigrants is added to the number of residents (offspring), we calculated the minimum percentage immigration after *t* generations as

$$P_{it} = P_{i0}\left(\frac{2}{3}\right)^t$$

2.11 | Annotation

The location of candidate SNPs was compared to the NCBI *Myotis Lucifugus* Annotation Release 102 (NCBI). This allowed us to identify SNPs located within known (or inferred) gene regions and unknown putative proteins. We then used the Ensembl Variant Effect predictor (McLaren et al., 2016) to identify the location of SNPs within genes (introns vs. exons).

3 | RESULTS

3.1 | Population trajectories

Demographic declines were dramatic within the smaller Hibernia colony, with an estimated population size of 26,438 individuals in 2009, declining by 98% to 495 individuals in 2015 (Figure 1b). Survival rates increased from 2010 to 2015, reaching pre-WNS

survival rates and slow but positive population growth at a rate of 1.03 by 2015 (Figure S3). At the larger Williams colony, steep but less dramatic declines from 87,401 individuals in 1999 to 16,673 individuals in 2010 (80% decline) were followed by partial recovery of the population abundance by 2015 (Figure 1b).

3.2 | Population structure and summary statistics

Whole genome sequencing on 132 individuals from four hibernacula collected at two time points (Figure 1a; Table S1) identified 31,517,948 SNPs. We found little geographical structure at a genome-wide level, including low pairwise F_{ST} values among nonsurvivor samples (0.0176 ± 0.000033) and among survivor samples (0.0143 ± 0.000333). In addition, the weak evidence for population structure that was identified with PCA and admixture analyses did not correspond to geography (Figure 2). Admixture proportions indicated that two of the bats from Williams may have originated from a second genetically distinct population (Figure 2b). To avoid potentially confounding population changes with signatures of selection, we removed these two bats, plus two other potentially genetically divergent bats (Figure 2a), from calculations of allele frequency for the results presented in the main paper, but also conducted the same analyses with all bats included as a sensitivity test (Figure S4). Relatedness estimates showed that all individuals are probably unrelated.

Overall, we also found little genome-wide temporal structure when we compared nonsurvivor samples to survivor samples from Hibernia (FST =0.016) or Williams (FST =0.017). We therefore do not find genetic evidence to suggest that nonsurvivor populations were replaced by individuals from other populations (Figure 2).

Hibernia and Williams differed in Tajima's *D* changes through time. Genome-wide average Tajima's *D* (±*SEM*) increased through time in Hibernia (from $-0.65 \pm 9.58 \times 10^{-5}$ to $-0.36 \pm 9.97 \times 10^{-5}$) and decreased slightly in Williams (from $-0.59 \pm 9.63 \times 10^{-5}$ to $-0.65 \pm 1.01 \times 10^{-6}$; Figure 3). We did not detect substantial changes in overall genetic diversity (π) through time (Table S1).

3.3 | Candidate SNPs under selection

To test for signals of selection in populations from Hibernia and Williams, we compared allele frequency changes through time against a null model of genetic drift and sampling error. Out of 242 SNPs with an absolute change in allele frequency greater than 0.5 in both populations, this approach identified 63 SNPs with significantly greater allele frequency changes than would be expected from the null model (hereafter referred to as candidate SNPs; Table S2, Figure S2; Figure 4a,b). The 242 SNPs with large allele frequency changes (>0.5) in both populations was more than the 44 (95% confidence interval 32–58) overlapping SNPs that would be expected if changes in the two populations were not happening in parallel.

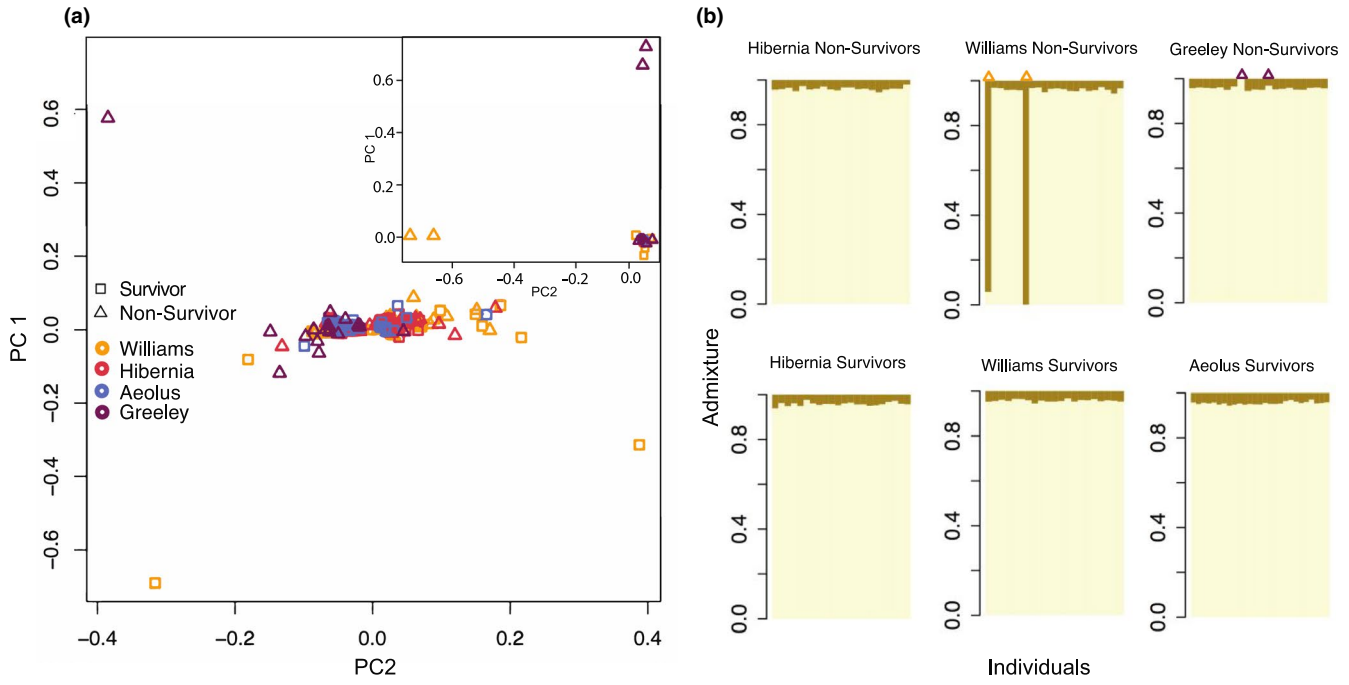

FIGURE 2 Lack of clear population structure of little brown bats in the northeastern United States across geography and time. (a) A PCA identified four potential genetically divergent bats (inset is the PCA conducted on all bats) and a lack of population structure in the majority of individuals (main figure is the PCA conducted after the four potentially divergent bats have been removed). MAP analysis identified only one significant principal component (PC 1). (b) Admixture plot showing two populations, which was the most probable value determined by MAP analysis. Note that all sites were analysed together and are only separated visually for clarity. Colours denote different inferred ancestral origin populations. The four potentially divergent bats from the PCA are marked at the top of the admixture plots

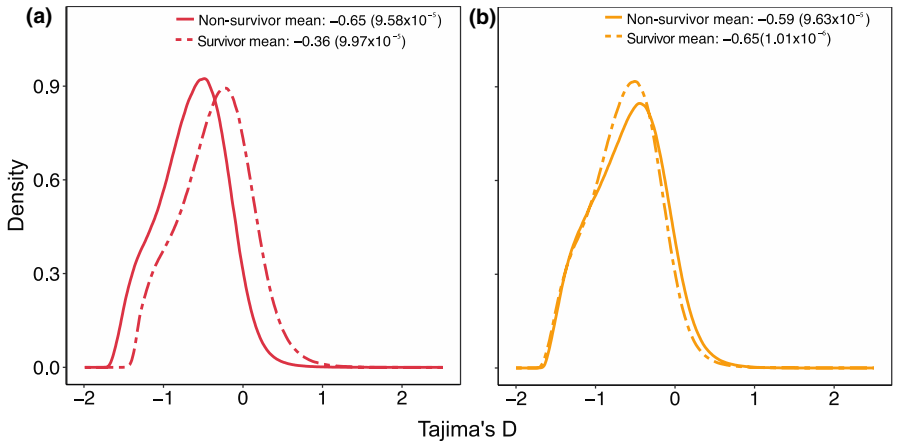

FIGURE 3 Change in Tajima's *D* in Hibernia and Williams. Density plots of Tajima's *D* calculated in sliding windows across the genome in (a) Hibernia and (b) Williams from nonsurvivors (solid line) and survivors (dotted line). Mean (*SE*) value of Tajima's *D* for every site sequenced across the entire genome is noted for each hibernaculum

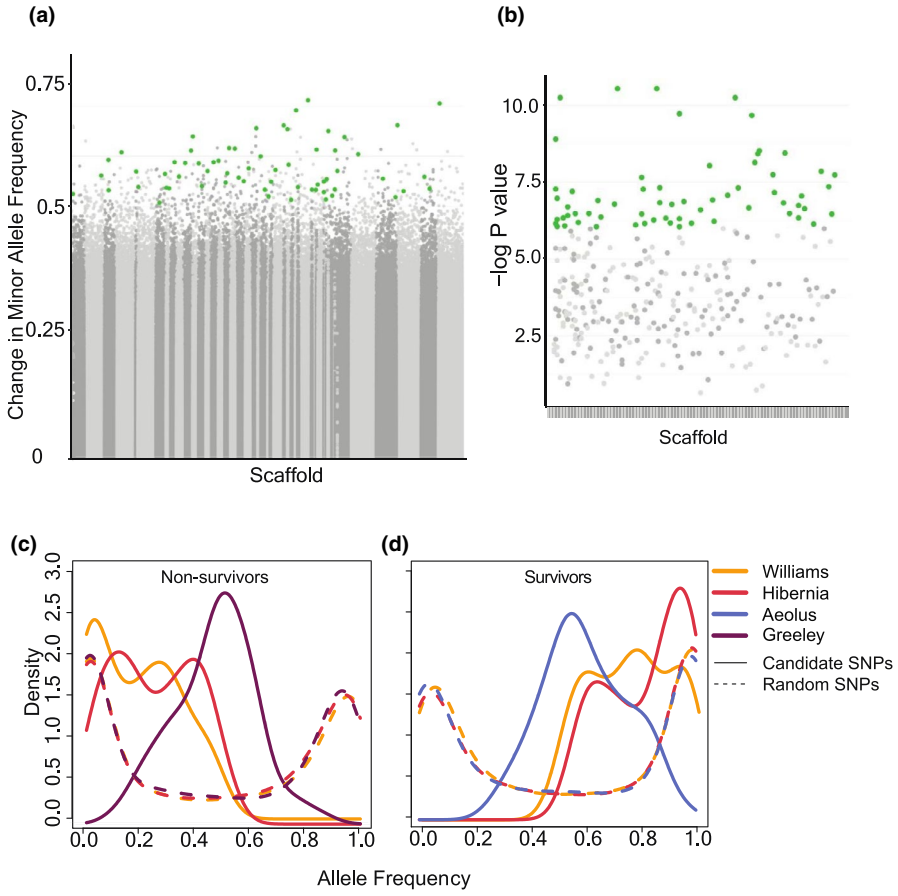

FIGURE 4 SNPs with signals of soft sweeps were located throughout the genome, were present at low to intermediate frequencies prior to white-nose syndrome (WNS) infection in all three populations, and swept to incomplete or nearly complete fixation after WNS in Hibernia and Williams. (a) Mean (Hibernia and Williams) change in allele frequency between nonsurvivor and survivor samples. Scaffolds are displayed in the order of the MyoLuc 2.0 assembly. Significant SNPs at a false discovery rate = 0.2 are highlighted in green. (b) Combined *p*-values across Hibernia and Williams for SNPs with a change in allele frequency greater than 0.5 in both Hibernia and Williams. Scaffolds are coloured along the *x* axis. Significant SNPs are highlighted in green. (c, d) Density plots of allele frequencies for significant candidate SNPs (solid lines) and for SNPs randomly chosen throughout the genome (dotted lines) at each site in (c) nonsurvivors and (d) survivors

In addition, we used a CMH test to identify potential SNPs of small effect (including SNPs with allele frequency changes less than 0.5) across both Hibernia and Williams. We identified 9615 significant SNPs, indicating that there is potential for considerable contributions by a large number of SNPs of small effect (Table S3). Forty-three of these SNPs overlapped with our candidate SNPs, providing further evidence of their importance (noted in Table S2).

For the candidate SNPs, all selected alleles were present at low to moderate frequencies (<0.6) in nonsurvivor populations from both Hibernia and Williams (Figure 4c). The nonzero starting allele frequencies are consistent with a soft selective sweep from standing genetic variation, a likely mode of selection given the short timescale of WNS infection, mortality and recovery. Survivor allele frequencies in Hibernia and Williams ranged from intermediate to high (>0.4), suggesting incomplete selective sweeps at some loci and near-complete sweeps at others (Figure 4d). As further evidence against hard sweeps, genomic regions surrounding candidate SNPs putatively under selection did not show classic signatures of hard sweeps, such as changes in π and Tajima's *D* (Figures S5 and S6).

We then conducted forward genetic simulations with selection, drift and sampling variance in an ABC framework to estimate which selection coefficients (*s*) would be consistent with the observed allele frequency changes at these 63 loci. Results suggested that these candidate SNPs experienced large selection

coefficients. Eleven mean posterior *s* values were >0.9 or <−0.9 in both Hibernia (mean absolute value of *s* of 0.81 across all 63 loci) and Williams (mean absolute value of *s* of 0.80) populations, consistent with strong selection acting on standing genetic variation (Table S2).

We further tested whether parallel changes in allele frequencies across Hibernia and Williams could be explained by dispersal between populations. However, we found that migrating individuals would have to make up >27% of each population (Table S4). Mark–recapture data collected at Hibernia over the last 7 years found that all bats banded at this hibernaculum were subsequently recaptured in later years, suggesting limited movement (Table S5). Furthermore, biannual surveys of Williams have shown that <0.02% of bats at Williams (out of 16,000) have been detected migrating from Hibernia. No bats from Williams have been found at Hibernia (Tables S6 and S4). This result suggests that selection acted *in situ* and largely independently in each population after WNS infection.

All candidate SNPs were present in samples from Greeley at intermediate allele frequencies (0.2–0.8), suggesting that they were available for selection (lack of survivor sampling means we cannot determine if selection occurred). Candidate allele frequencies at Aeolus were also mostly intermediate (0.2–0.8) with only a few at high frequencies (0.8–1; Figure 4c,d), which suggests that—while some degree of parallel selection is occurring across sampled populations—selection is not acting to the same degree on the same loci in all populations affected by WNS.

Sixteen of the 63 candidate SNPs putatively under selection were located in annotated regions of the genome (Table S2). No gene contained more than one SNP and all SNPs were located in presumed introns. *KREMEN1* contained the SNP with the highest absolute *s* value of 0.94 (averaged between Hibernia and Williams), with *MASP1*, *FBXL17* and *CMIP* all containing SNPs with an average *s* value of 0.93.

4 | DISCUSSION

Pathogen-induced mass mortalities provide natural experiments to study selection and the potential for evolutionary rescue of wild populations. To examine both the population genetic effects of WNS-induced mortalities and genetic signatures that may be associated with resistance, we collected samples from two hibernacula where population sizes have been closely monitored and populations are showing signs of recovery. By pairing samples of survivors and nonsurvivors from the same hibernacula, we were able to examine changes in allele frequencies through time. Populations did not show large genome-wide changes, but rather subtle signatures of soft selective sweeps from standing genetic variation. We identified 63 candidate SNPs under selection shared between two populations exhibiting recovery from WNS-induced declines. These SNPs were located in genes associated with immunity, metabolism and hibernation, consistent with the effects of WNS on hibernating bats.

4.1 | Population structure

The observed lack of population structure is consistent with previous studies demonstrating near-panmixia over evolutionary time in bat populations east of the Rocky Mountains (Vonhof et al., 2015; Wilder et al., 2015), probably because even a small number of bats moving between hibernacula reduces population structure on an evolutionary timescale (Waples & Gaggiotti, 2006). Despite near-panmixia over evolutionary time, most bats have fidelity to mating sites and hibernacula on ecological timescales (Norquay et al., 2013). Our own mark–recapture work found that all bats banded at Hibernia were resighted at Hibernia at least once, with several resighted every year post-banding.

4.2 | Genetic signatures of population change

While both Hibernia and Williams populations are currently recovering, they experienced different rates of decline and subsequent growth that can leave genetic signatures. Tajima's *D* is a genetic statistic that typically increases during a population bottleneck as rare variants are lost (and intermediate frequency alleles become more common), with the strongest effects in populations that reach the smallest sizes (Tajima, 1989). Tajima's *D* increased through time in the smaller Hibernia site where populations declined more dramatically, suggesting that the population is currently experiencing the effects of a recent genetic bottleneck. In contrast, Tajima's *D* decreased slightly in the relatively more abundant and rapidly recovering Williams population, suggesting that this population did not experience as strong a genetic bottleneck due to its larger population size.

4.3 | Genetic signatures of selection

WNS-induced population declines were sudden and dramatic, leaving little opportunity for host evolution of tolerance or resistance through de novo mutation. The 63 candidate SNPs identified here display signatures consistent with soft sweeps from standing genetic variation, a mode of rapid evolution that is important, poorly understood and often challenging to detect (Messer & Petrov, 2013; Przeworski et al., 2005). Signatures of soft sweeps can be easily obscured by geographical variation in allele frequencies. We used an approach that has successfully detected disease-induced selection in other systems (Schiebelhut et al., 2018): collecting samples from the same geographical sites at different time points allowed us to track changes in allele frequencies within populations. However, because our early samples were collected only from nonsurvivors, they do not give us a precise estimate of allele frequencies in the pre-WNS population. It is possible that alleles at low frequencies in the nonsurvivors may have been at higher frequencies in the pre-WNS population, but were maladaptive, which would cause our methods to over-estimate

selection strengths. However, most of the pre-WNS population died, which implies that the frequencies in the nonsurvivors cannot have been substantially different from frequencies in the total pre-WNS population.

We were able to detect signatures of selection within introns, which generally have higher diversity due to lower evolutionary constraint and may be good candidates for selection on standing genetic variation. While often overlooked as targets of selection, introns can play important regulatory roles, and mutations in introns have been associated with numerous diseases (Ma et al., 2015). Promoter regions in particular appear to play an important role in disease (Ma et al., 2015), which would be a promising area for future research regarding WNS. Interestingly, some of the candidate SNPs show a decay in π and Tajima's *D* with distance, suggesting that we are identifying selection in areas of the genome with increased polymorphism. This may be caused by Copy Number Variations (CNVs) or historical balancing selection, although further investigation is needed to understand these patterns and definitively rule out alternative explanations (e.g., mapping error).

These 63 identified SNPs are not meant to be representative of all SNPs under selection by WNS. Our conservative approach and decision to focus on SNPs with large changes in allele frequency helped to reduce false positives but also probably resulted in this analysis missing many additional SNPs under selection (see Figure S2). We found that more stringent quality filters did not have a considerable effect on allele frequencies (Figure S1) and that a higher *q* value served to balance out the problem of false negatives (Figure S2). Our finding that 9615 SNPs have significant changes in allele frequency between survivor and nonsurvivor populations provides evidence that many SNPs of potentially small effect may be involved in survival (Table S3). These SNPs would be promising targets for further investigation. Furthermore, soft sweeps from standing genetic variation will be heavily affected by the pre-existing genetic makeup of a given population, making variation in targets of selection across populations highly likely (Yeaman, 2015). Sampling nonsurvivors from the initial wave of WNS mortality means that we were not able to fully characterize the predisease allele frequencies, although the lack of fixed differences between pre- and post-disease populations made clear that any adaptive variation is not fully protective from WNS. Our finding that putatively adaptive alleles were present in nonsurvivors suggests that these samples contained an acceptable part of the population diversity. Differences in the strength and nature of selective pressures can result from differences in overall climate and microclimates between hibernacula, which were not collected as part of this study (Langwig et al., 2012). In fact, our finding that allele frequencies in the two Vermont hibernacula did not follow the patterns found at Hibernia and Williams suggests that selection is operating differently in different populations. Three recent studies of *Myotis lucifugus* have compared nonsurvivors and survivors (or pre- and post-WNS) in Michigan (Auteri & Knowles, 2020), Canada (Ontario, Manitoba, Nova Scotia and Prince Edward Island; Donaldson et al., 2017) and the Mid-Atlantic (Pennsylvania and New York; Lilley et al., 2020). There is no overlap between studies (including this study) in the genes that contain signatures of selection, possibly due to selection acting on different standing genetic variation in different groups of bats. Importantly, none of the previous studies sampled the same hibernacula over time, but rather were comparing allele frequencies of combined samples collected from multiple sites. Lilley et al. (2020) found significant divergence of post-WNS bats in New York and Pennsylvania at certain regions of the genome and suggested that some of this divergence could mask more subtle signatures of selection. However, limits within each study mean that it is not yet clear whether the different sets of candidate loci arise because of limited statistical power and false negatives in each study or because the targets of selection are truly different. Differences in sequencing strategies (RAD-Seq (Auteri & Knowles, 2020), immunome targeted sequencing (Donaldson et al., 2017), whole genome sequencing (Lilley et al., 2020), this study) mean that overlap in the tested genomic regions was limited. In addition, because we sampled from populations that are currently recovering, our candidate SNPs may be more closely linked to evolved resistance than those identified by studies of populations that are continuing to decline.

A recent study compared the transcriptomes of infected and uninfected *M. lucifiugus* during and after torpor and found significantly more differentially expressed genes (between infected and uninfected bats) after arousal (Field et al., 2018). This work supports previous findings that while infection occurs during hibernation, the host response, development of severe disease signs and mortality occur only after arousal (Meteyer et al., 2012). Two of the genes containing candidate SNPs (*PCDH17* and *REPS2*) had higher levels of expression in infected than uninfected bats only after arousal from torpor, suggesting that they may play a role in disease progression within the wing. *PCDH17* is a protocadherin, a group of proteins that are best understood in the brain where they play important roles in development and maintenance of cell–cell junctions (Weiner & Jontes, 2013). Its potential role in wing tissue is unknown. *REPS2* is a part of the Ras/Ral signalling pathway, which is important for receptor-mediated endocytosis (Badway & Baleja, 2011). None of the genes identified by previous studies of WNS-induced selection (Auteri & Knowles, 2020; Donaldson et al., 2017; Lilley et al., 2020) were differentially expressed between infected and uninfected bats. Taken together, our study and Field *et al.* (2018) provide strong evidence that *PCDH17* and *REPS2* may be involved in the host response to *Pseudogymnoascus destructans* and should be further investigated as genes associated with resistance.

Pathogen-induced selection is often focused on genes associated with the host immune system (e.g., Alves et al., 2019; Epstein et al., 2016). However, the role of the immune system in WNS pathology and resistance remains unclear, as activation of the immune system is not the immediate response of hibernating bats infected with *P. destructans* nor is it directly related to bat mortality (Lilley et al., 2017; Reeder et al., 2012). Furthermore, our understanding of immune system activation is complicated

by immune suppression during hibernation (Sahdo et al., 2013). Adaptive immunity does not seem to be the primary mechanism of WNS resistance as production of anti-*P. destructans* antibodies has no effect on survival outcome of infected *M. lucifugus* (Lilley et al., 2017). In fact, the production of antibodies may be maladaptive because infected European bats displaying no signs of WNS frequently have lower levels of anti-*P. destructans* antibodies than uninfected bats (Johnson et al., 2015). In addition, big brown bats (*Eptesicus fuscus*), which have suffered much smaller population declines from WNS, appear to mount a targeted immune response localized to WNS lesions, contrasting with the systemic response of *M. lucifugus* (Davy et al., 2020). Donaldson et al. (2017) found sequence variation in 138 immune genes including members of the Toll pathway, interleukins and MHCs, some of which differed between WNS-exposed and unexposed populations. We found one candidate SNP in a gene involved in the innate immune system (*MASP1*, part of the lectin pathway of the complement system). *MASP1* cleaves C4 and C2 to create C3 convertase, which then cleaves complement component C3 (Moller-Kristensen et al., 2007). Levels of complement component C3 were recently found to be higher in the blood plasma of infected hibernating *M. lucifugus* than uninfected *M. lucifugus* (Hecht-Hoger et al., 2020). Hibernation also influences the complement system: antipathogen presumed complement activity was reduced in hibernating *M. lucifugus* (Moore et al., 2011) and *MASP1* is less abundant in brown bears during hibernation (Welinder et al., 2016). Selection on innate immune genes could be due to an adaptive role in WNS resistance or a maladaptive role in WNS-induced mortality.

Instead of immunity, a key target of selection appears to be genes related to hibernation and metabolism. WNS-infected bats exhibit an increase in the frequency of torpor arousal and altered metabolism (Verant et al., 2014), which prematurely depletes fat stores and leads to mortality (Reeder et al., 2012; Verant et al., 2014). While the exact cause of these disease-induced changes in arousal patterns is unclear, increased arousal may be a failed attempt to fight off the pathogen by re-activating the immune system (Storey & Storey, 2004). Intriguingly, big brown bats, which have suffered much smaller population declines from WNS, increase (not shorten) their torpor duration when exposed to *P. destructans*, suggesting that differences in hibernation in addition to immune function play a role in disease resistance (Moore et al., 2018). Hibernating bats undergo significant changes in insulin levels, fat accumulation and metabolism throughout the hibernation cycle (Bauman, 1990; Carey et al., 2003). Two of the genes containing candidate SNPs have been directly tied to metabolism during hibernation (*ADCY3* and *RAPGEF1*). *ADCY3*, which in humans is associated with obesity (Grarup et al., 2018; Saeed et al., 2018; Stergiakouli et al., 2014), was found to be highly enriched in the brown adipose tissue of the 13-lined ground squirrel (Hampton et al., 2013). Brown adipose tissue provides an immediate energy source to hibernating mammals during interbout arousals (Hampton et al., 2013). *RAPGEF1*, which is involved in insulin signalling (Qu et al., 2011), was expressed in white adipose tissue (the main source of energy during hibernation) of Syrian hamsters upon initiation of torpor (Chayama et al., 2018). Further research will be needed to test the link between *ADCY3* and *RAPGEF1* in little brown bats and changes in hibernation phenotypes. Three other genes containing candidate SNPs (*CMIP* (Keaton et al., 2018), *REPS2* (Badway & Baleja, 2011), and *SOX5* (Axelsson et al., 2017)) have all been shown to play a role in insulin regulation in humans. Both Auteri and Knowles (2020) and Lilley et al. (2020) also found SNPs putatively under selection in genes associated with hibernation and metabolism, suggesting that hibernation behaviour plays a key role in WNS resistance.

Evolutionary rescue can allow for population persistence after an environmentally induced steep demographic decline if the decline is coupled with selection of more fit individuals. Observed population trajectories, as well as recent demographic analyses (Maslo et al., 2015; Fig S1), suggest that surviving individuals may have the potential to rescue little brown bat populations and ultimately return them to stable population levels (Maslo & Fefferman, 2015). Our results suggest that little brown bat populations are experiencing a disease-induced selection event, which could be responsible for the positive growth of these populations through evolutionary rescue. However, further experimental work testing for differences in survival of infected individuals with different alleles is needed to directly tie genetic changes to increased fitness. Furthermore, characterizing the full suite of adaptive alleles present will require detecting SNPs probably under selection in other populations given that differences in pre-WNS genetic variation determines which alleles are available for selection and which genetic background they act within. To most accurately detect subtle signatures of selection, future work on other populations should involve comparing samples from single populations over time and then comparing across populations. Ultimately, management decisions (e.g., whether to deploy treatments for *P. destructans* or to protect populations from other detrimental factors) can be informed by knowing the frequency of resistant individuals in both uninfected and infected populations. The deployment of vaccines or treatments for *P. destructans* may be most needed in populations with low evolutionary potential (Maslo et al., 2017). This study documents pathogen-induced selection in recovering populations, a necessary step towards understanding whether evolutionary rescue is occurring. By closely observing wild populations of nonmodel organisms, we can document unique natural experiments that help to expand our understanding of how and when natural selection occurs.

ACKNOWLEDGEMENTS

The authors would like to thank Nina Therkildsen, Noah Rose, Ryan Waples, Michelle Stuart and Wei Wang for help with troubleshooting; Chris Gignoux, Lisa Komoroske, Jennifer Hoey, Katrina Catalano, Winifred Frick, A. Marm Kilpatrick, Erik Holum and Thomas Lilley for discussions about bat ecology and data analyses; and Chris Gignoux, Lacey Knowles and Katrina Lohan for reviewing a draft manuscript. We thank Brian Schumm and other field

personnel for assistance in sampling bats. Funding for this project was provided through United States Fish and Wildlife Service Grant F15AP00949 and US National Science Foundation grant #OCE-1426891.

AUTHOR CONTRIBUTIONS

B.M., M.P. and N.F. conceived the project, B.M., K.K., C.H., M.H. and A.B. performed sample collection, S.G.W. conducted all laboratory work and data analysis with input from B.M. and M.P., and S.G.W. wrote the manuscript with input from all coauthors.

DATA AVAILABILITY STATEMENT

Sequences are available from the NCBI Short Read Archive (Bioproject PRJNA509256, accession nos. SAMN10574961–SAMN10575092). All scripts and notebooks are publicly available in a GitHub repository archived on Zenodo with https://doi.org/10.5281/zenodo.4433006.

ORCID

Sarah A. Gignoux-Wolfsohn https://orcid.org/0000-0002-9037-1088
Malin L. Pinsky https://orcid.org/0000-0002-8523-8952
Brooke Maslo https://orcid.org/0000-0003-3847-3164

REFERENCES

Alex Buerkle, C., & Gompert, Z. (2013). Population genomics based on low coverage sequencing: How low should we go? *Molecular Ecology*, *22*(11), 3028–3035. https://doi.org/10.1111/mec.12105

Alves, J. M., Carneiro, M., Cheng, J. Y., Lemos de Matos, A., Rahman, M. M., Loog, L., Campos, P. F., Wales, N., Eriksson, A., Manica, A., Strive, T., Graham, S. C., Afonso, S., Bell, D. J., Belmont, L., Day, J. P., Fuller, S. J., Marchandeau, S., Palmer, W. J., … Jiggins, F. M. (2019). Parallel adaptation of rabbit populations to myxoma virus. *Science*, *363*, 1319–1326.

Anderson, E. C., Skaug, H. J., & Barshis, D. J. (2014). Next-generation sequencing for molecular ecology: A caveat regarding pooled sampled. *Molecular Ecology*, *23*, 502–512.

Auteri, G. G., & Knowles, L. L. (2020). Decimated little brown bats show potential for adaptive change. *Scientific Reports*, *10*(1), 3023. https://doi.org/10.1038/s41598-020-59797-4

Axelsson, A. S., Mahdi, T., Nenonen, H. A., Singh, T., Hänzelmann, S., Wendt, A., Bagge, A., Reinbothe, T. M., Millstein, J., Yang, X., Zhang, B., Gusmao, E. G., Shu, L., Szabat, M., Tang, Y., Wang, J., Salö, S., Eliasson, L., Artner, I., … Rosengren, A. H. (2017). Sox5 regulates beta-cell phenotype and is reduced in type 2 diabetes. *Nature Communications*, *8*, 15652. https://doi.org/10.1038/ncomms15652

Badway, J. A., & Baleja, J. D. (2011). Reps2: A cellular signaling and molecular trafficking nexus. *The International Journal of Biochemistry & Cell Biology*, *43*(12), 1660–1663. https://doi.org/10.1016/j.biocel.2011.08.014

Bauman, W. A. (1990). Seasonal changes in pancreatic insulin and glucagon in the little brown bat. *Pancreas*, *5*(3), 342–346.

Baym, M., Kryazhimskiy, S., Lieberman, T. D., Chung, H., Desai, M. M., & Kishony, R. (2015). Inexpensive multiplexed library preparation for megabase-sized genomes. *Plos one*, *10*(5), e0128036. https://doi.org/10.1371/journal.pone.0128036

Beaumont, M. A., Zhang, W., & Balding, D. J. (2002). Approximate Bayesian computation in population genetics. *Genetics*, *162*, 2025–2035.

Burge, C. A., Mark Eakin, C., Friedman, C. S., Froelich, B., Hershberger, P. K., Hofmann, E. E., Petes, L. E., Prager, K. C., Weil, E., Willis, B. L., Ford, S. E., & Harvell, C. D. (2014). Climate change influences on marine infectious diseases: Implications for management and society. *Annual Review of Marine Science*, *6*, 249–277. https://doi.org/10.1146/annurev-marine-010213-135029

Burnham, K. P., & Anderson, D. R. (2002). *Model selection and multimodel inference: A practical information-theoretic approach*. Springer.

Burnham, K. P., Anderson, D. R., & Huyvaert, K. P. (2011). AIC model selection and multimodel inference in behavioral ecology: Some background, observations, and comparisons. *Behavioral Ecology and Sociobiology*, *65*(1), 23–35.

Carey, H. V., Andrews, M. T., & Martin, S. L. (2003). Mammalian Hibernation: Cellular and molecular responses to depressed metabolism and low temperature. *Physiological Reviews*, *83*, 1153–1181.

Chayama, Y., Ando, L., Sato, Y., Shigenobu, S., Anegawa, D., Fujimoto, T., Taii, H., Tamura, Y., Miura, M., & Yamaguchi, Y. (2018). Molecular basis of white adipose tissue remodeling that precedes and coincides with hibernation in the Syrian hamster, a food-storing hibernator. *Frontiers in Physiology*, *9*, 1973. https://doi.org/10.3389/fphys.2018.01973

Conover, D., Clarke, L., Munch, S., & Wagner, G. (2006). Spatial and temporal scales of adaptive divergence in marine fishes and the implications for conservation. *Journal of Fish Biology*, *69*, 21–47.

Csillery, K., Blum, M. G., Gaggiotti, O. E., & Francois, O. (2010). Approximate Bayesian Computation (ABC) in practice. *Trends in Ecology & Evolution*, *25*(7), 410–418. https://doi.org/10.1016/j.tree.2010.04.001

Cutler, D. J., & Jensen, J. D. (2010). To pool, or not to pool? *Genetics*, *186*(1), 41–43. https://doi.org/10.1534/genetics.110.121012

Darimont, C. T., Carlson, S. M., Kinnison, M. T., Paquet, P. C., Reimchen, T. E., & Wilmers, C. C. (2009). Human predators outpace other agents of trait change in the wild. *Proceedings of the National Academy of Sciences*, *106*(3), 952–954.

Davy, C. M., Donaldson, M. E., Bandouchova, H., Breit, A. M., Dorville, N. A. S., Dzal, Y. A., Kovacova, V., Kunkel, E. L., Martínková, N., Norquay, K. J. O., Paterson, J. E., Zukal, J., Pikula, J., & Willis, C. K. R. & Kyle, C. J. (2020). Transcriptional host–pathogen responses of *Pseudogymnoascus destructans* and three species of bats with white-nose syndrome. *Virulence*, *11*(1), 781–794. https://doi.org/10.1080/21505594.2020.1768018

Derrien, T., Estelle, J., Marco Sola, S., Knowles, D. G., Raineri, E., Guigo, R., & Ribeca, P. (2012). Fast computation and applications of genome mappability. *PLoS One*, *7*(1), e30377. https://doi.org/10.1371/journal.pone.0030377

Donaldson, M. E., Davy, C. M., Willis, C. K. R., McBurney, S., Park, A., & Kyle, C. J. (2017). Profiling the immunome of little brown myotis provides a yardstick for measuring the genetic response to white-nose syndrome. *Evolutionary Applications*, *10*(10), 1076–1090. https://doi.org/10.1111/eva.12514

Epstein, B., Jones, M., Hamede, R., Hendricks, S., McCallum, H., Murchison, E. P., Schönfeld, B., Wiench, C., Hohenlohe, P., & Storfer, A. (2016). Rapid evolutionary response to a transmissible cancer in Tasmanian devils. *Nature Communications*, *7*, 12684. https://doi.org/10.1038/ncomms12684

Field, K. A., Sewall, B. J., Prokkola, J. M., Turner, G. G., Gagnon, M. F., Lilley, T. M., Paul White, J., Johnson, J. S., Hauer, C. L., & Reeder, D. A. M. (2018). Effect of torpor on host transcriptomic responses to a fungal pathogen in hibernating bats. *Molecular Ecology*, *27*, 3727–3743. https://doi.org/10.1111/mec.14827

Fisher, R. A. (1922). On the dominance ratio. *Proceedings of the Royal Society Edinburgh*, *42*, 321–431.

Frick, W., Cheng, T. L., Langwig, K. E., Hoyt, J. R., Janicki, A. F., Parise, K. L., Foster, J. T., & Kilpatrick, A. M. (2017). Pathogen dynamics during invasion and establishment of white-nose syndrome explain mchanisms of host persistence. *Ecology*, *98*(3), 624–631.

Frick, W. F., Pollock, J. F., Hicks, A. C., Langwig, K. E., Reynolds, D. S., Turner, G. G., Butchkoski, C. M., & Kunz, T. H. (2010). An emerging disease causes regional population collapse of a common North American bat species. *Science*, *329*(5992), 679–682. https://doi.org/10.1126/science.1188594

Frick, W. F., Puechmaille, S. J., Hoyt, J. R., Nickel, B. A., Langwig, K. E., Foster, J. T., Barlow, K. E., Bartonička, T., Feller, D., Haarsma, A.-J., Herzog, C., Horáček, I., van der Kooij, J., Mulkens, B., Petrov, B., Reynolds, R., Rodrigues, L., Stihler, C. W., Turner, G. G., & Kilpatrick, A. M. (2015). Disease alters macroecological patterns of North American bats. *Global Ecology and Biogeography*, *24*(7), 741–749. https://doi.org/10.1111/geb.12290

Frick, W. F., Reynolds, D. S., & Kunz, T. H. (2010). Influence of climate and reproductive timing on demography of little brown myotis *Myotis lucifugus*. *Journal of Animal Ecology*, *79*(1), 128–136. https://doi.org/10.1111/j.1365-2656.2009.01615.x

Gargas, A., Trest, M. T., Christensen, M., Volk, T. J., & Blehert, D. S. (2009). *Geomyces destructans* sp. nov. associated with bat white-nose syndrome. *Mycotaxon*, *108*, 147–154.

Grarup, N., Moltke, I., Andersen, M. K., Dalby, M., Vitting-Seerup, K., Kern, T., Mahendran, Y., Jørsboe, E., Larsen, C. V. L., Dahl-Petersen, I. K., Gilly, A., Suveges, D., Dedoussis, G., Zeggini, E., Pedersen, O., Andersson, R., Bjerregaard, P., Jørgensen, M. E., Albrechtsen, A., & Hansen, T. (2018). Loss-of-function variants in ADCY3 increase risk of obesity and type 2 diabetes. *Nature Genetics*, *50*(2), 172–174. https://doi.org/10.1038/s41588-017-0022-7

Hampton, M., Melvin, R. G., & Andrews, M. T. (2013). Transcriptomic analysis of brown adipose tissue across the physiological extremes of natural hibernation. *PLoS One*, *8*(12), e85157. https://doi.org/10.1371/journal.pone.0085157

Hecht-Hoger, A. M., Braun, B. C., Krause, E., Meschede, A., Krahe, R., Voigt, C. C., Greenwood, A. D., & Czirjak, G. A. (2020). Plasma proteomic profiles differ between European and North American myotid bats colonized by Pseudogymnoascus destructans. *Molecular Ecology*, *29*, 1745–1755. https://doi.org/10.1111/mec.15437

Herzog, C. New York State Department of Environmental Conservation (unpublished data).

Johnson, J. B., & Omland, K. S. (2004). Model selection in ecology and evolution. *Trends in Ecology & Evolution*, *19*, 101–108.

Johnson, J. S., Reeder, D. M., Lilley, T. M., Czirják, G. Á., Voigt, C. C., McMichael, J. W., Seery, C. W., Lumadue, S. S., Altmann, A. J., Toro, M. O., & Field, K. A. (2015). Antibodies to *Pseudogymnoascus destructans* are not sufficient for protection against white-nose syndrome. *Ecology and Evolution*, *5*(11), 2203–2214. https://doi.org/10.1002/ece3.1502

Keaton, J. M., Gao, C., Guan, M., Hellwege, J. N., Palmer, N. D., Pankow, J. S., Fornage, M., Wilson, J. G., Correa, A., Rasmussen-Torvik, L. J., Rotter, J. I., Chen, Y. I., Taylor, K. D., Rich, S. S., Wagenknecht, L. E., Freedman, B. I., Ng, M. C. Y., & Bowden, D. W. (2018). Genome-wide interaction with the insulin secretion locus MTNR1B reveals CMIP as a novel type 2 diabetes susceptibility gene in African Americans. *Genetic Epidemiology*, *42*(6), 559–570. https://doi.org/10.1002/gepi.22126

Keen, R., & Hitchcock, H. B. (1980). Survival and longevity of the little brown bat (*Myotis lucifugus*) in Southeastern Ontario. *Journal of Mammalogy*, *61*(1), 1–7.

Korneliussen, T. S., Albrechtsen, A., & Nielsen, R. (2014). ANGSD: Analysis of next generation. Sequencing data. *BMC Bioinformatics*, *15*(356).

Kunz, T. H., & Reichard, J. D. (2010). *Status review of the little brown myotis (*Myotis lucifugus*) and determination that immediate listing under the Endangered Species Act is scientifically and legally warranted*. Retrieved from Boston MA.

Langmead, B., & Salzberg, S. L. (2012). Fast gapped-read alignment with Bowtie 2. *Nature Methods*, *9*(4), 357–359. https://doi.org/10.1038/nmeth.1923

Langwig, K. E., Frick, W. F., Bried, J. T., Hicks, A. C., Kunz, T. H., & Kilpatrick, A. M. (2012). Sociality, densitydependence and microclimates determine the persistence of populations suffering from a novel fungal disease, white-nose syndrome. *Ecol Lett*, *15*(9), 1050–1057. https://doi.org/10.1111/j.1461-0248.2012.01829

Langwig, K. E., Hoyt, J. R., Parise, K. L., Frick, W. F., Foster, J. T., & Kilpatrick, A. M. (2017). Resistance in persisting bat populations after white-nose syndrome invasion. *Philosophical Transactions of the Royal Society of London. Series B, Biological Sciences*, *372*(1712). https://doi.org/10.1098/rstb.2016.0044

Lilley, T. M., Prokkola, J. M., Johnson, J. S., Rogers, E. J., Gronsky, S., Kurta, A., Reeder, D. M., & Field, K. A. (2017). Immune responses in hibernating little brown myotis (*Myotis lucifugus*) with white-nose syndrome. *Proceedings of the Royal Society B: Biological Sciences*, *284*(1848), 20162232. https://doi.org/10.1098/rspb.2016.2232

Lilley, T. M., Wilson, I. W., Field, K. A., Reeder, D. M., Vodzak, M. E., Turner, G. G., Kurta, A., Blomberg, A. S., Hoff, S., Herzog, C. J., Sewall, B. J., & Paterson, S. (2020). Genome-wide changes in genetic diversity in a population of *Myotis lucifugus* affected by white-nose syndrome. *G3*, *10*, 2007–2020. https://doi.org/10.1534/g3.119.400966

Ma, M., Ru, Y., Chuang, L.-S., Hsu, N.-Y., Shi, L.-S., Hakenberg, J., Cheng, W.-Y., Uzilov, A., Ding, W., Glicksberg, B. S., & Chen, R. (2015). Disease-associated variants in different categories of disease located in distinct regulatory elements. *BMC Genomics*, *16*(53).

Maslo, B., & Fefferman, N. H. (2015). A case study of bats and white-nose syndrome demonstrating how to model population viability with evolutionary effects. *Conservation Biology*, *29*(4), 1176–1185. https://doi.org/10.1111/cobi.12485

Maslo, B., Gignoux-Wolfsohn, S., & Fefferman, N. H. (2017). Success of wildlife disease treatment depends on host immune response. *Frontiers in Ecology and Evolution*. https://doi.org/10.3389/fevo.2017.00028

Maslo, B., Valent, M., Gumbs, J. F., & Frick, W. (2015). Conservation implications of ameliorating survival of little brown bats with white-nose syndrome. *Ecological Applications*, *25*(7), 1832–1840.

McLaren, W., Gil, L., Hunt, S. E., Riat, H. S., Ritchie, G. R. S., Thormann, A., Flicek, P., & Cunningham, F. (2016). The Ensembl variant effect predictor. *Genome Biology*, *17*(1). https://doi.org/10.1186/s13059-016-0974-4.

Meisner, J., & Albrechtsen, A. (2018). *Inferring population structure and admixture proportions in low depth NGS data*. doi: https://doi.org/10.1101/302463

Messer, P. W., & Petrov, D. A. (2013). Population genomics of rapid adaptation by soft selective sweeps. *Trends in Ecology & Evolution*, *28*(11), 659–669. https://doi.org/10.1016/j.tree.2013.08.003

Meteyer, C. U., Barber, D., & Mandl, J. N. (2012). Pathology in euthermic bats with white nose syndrome suggests a natural manifestation of immune reconstitution inflammatory syndrome. *Virulence*, *3*(7), 583–588. https://doi.org/10.4161/viru.22330

Mikheyev, A. S., Tin, M. M., Arora, J., & Seeley, T. D. (2015). Museum samples reveal rapid evolution by wild honey bees exposed to a novel parasite. *Nature Communications*, *6*, 7991. https://doi.org/10.1038/ncomms8991

Moller-Kristensen, M., Thiel, S., Sjoholm, A., Matsushita, M., & Jensenius, J. C. (2007). Cooperation between MASP-1 and MASP-2 in the generation of C3 convertase through the MBL pathway. *International Immunology*, *19*(2), 141–149. https://doi.org/10.1093/intimm/dxl131

Moore, M. S., Field, K. A., Behr, M. J., Turner, G. G., Furze, M. E., Stern, D. W. F., Allegra, P. R., Bouboulis, S. A., Musante, C. D., Vodzak, M. E., Biron, M. E., Meierhofer, M. B., Frick, W. F., Foster, J. T., Howell, D., Kath, J. A., Kurta, A., Nordquist, G., Johnson, J. S., … Reeder, D. M. (2018). Energy conserving thermoregulatory patterns and lower disease severity in a bat resistant to the impacts of white-nose syndrome. *Journal of Comparative Physiology B*, *188*, 163–176. https://doi.org/10.1007/s00360-017-1109-2

Moore, M. S., Reichard, J. D., Murtha, T. D., Zahedi, B., Fallier, R. M., & Kunz, T. H. (2011). Specific alterations in complement protein activity of little brown myotis (*Myotis lucifugus*) hibernating in white-nose syndrome affected sites. *PLoS One*, *6*(11), e27430. https://doi.org/10.1371/journal.pone.0027430

National White-nose Syndrome Decontamination Protocols. Retrieved from https://s3.amazonaws.com/org.whitenosesyndrome.assets/prod/7a93cc80-b785-11e8-87bb-317452edc988-National_WNS_Decon_UPDATE_09132018.pdf

NCBI. Retrieved from https://www.NCBI.nlm.nih.gov/genome/annotation_euk/Myotis_lucifugus/102/.

Nielsen, R., Korneliussen, T., Albrechtsen, A., Li, Y., & Wang, J. (2012). SNP calling, genotype calling, and sample allele frequency estimation from New-Generation Sequencing data. *PLoS One*, *7*(7), e37558. https://doi.org/10.1371/journal.pone.0037558

Norquay, K. J. O., Martinez-Nuñez, F., Dubois, J. E., Monson, K. M., & Willis, C. K. R. (2013). Long-distance movements of little brown bats (*Myotis lucifugus*). *Journal of Mammalogy*, *94*(2), 506–515. https://doi.org/10.1644/12-mamm-a-065.1

North, B. V., Curtis, D., & Sham, P. C. (2002). A note on the calculation of empirical P values from Monte Carlo procedures. *American Journal of Human Genetics*, *71*(2), 439–441. https://doi.org/10.1086/341527

Oziolor, E. M., Reid, N. M., Yair, S., Lee, K. M., Guberman VerPloeg, S., Bruns, P. C., Shaw, J. R., Whitehead, A., & Matson, C. W. (2019). Adaptive introgression enables evolutionary rescue from extreme environmental pollution. *Science*, *364*, 455–457.

Prince, D. J., O'Rourke, S. M., Thompson, T. Q., Ali, O. A., Lyman, H. S., Saglam, I. K., Hotaling, T. J., Spidle, A. P., & Miller, M. R. (2017). The evolutionary basis of premature migration in pacific salmon highlights the utility of genomics for informing conservation. *Science Advances*, *3*, e1603198.

Przeworski, M., Coop, G., & Wall, J. D. (2005). The signature of positive selection on standing genetic variation. *Evolution*, *59*(11), 2312. https://doi.org/10.1554/05-273.1

Qu, L., He, B., Pan, Y., Xu, Y., Zhu, C., Tang, Z., Bao, Q., Tian, F., & Wang, S. (2011). Association between polymorphisms in RAPGEF1, TP53, NRF1 and type 2 diabetes in Chinese Han population. *Diabetes Research and Clinical Practice*, *91*(2), 171–176. https://doi.org/10.1016/j.diabres.2010.11.019

Quinlan, A. R., & Hall, I. M. (2010). BEDTools: A flexible suite of utilities for comparing genomic features. *Bioinformatics*, *26*(6), 841–842. https://doi.org/10.1093/bioinformatics/btq033

Reeder, D. A. M., Frank, C. L., Turner, G. G., Meteyer, C. U., Kurta, A., Britzke, E. R., Vodzak, M. E., Darling, S. R., Stihler, C. W., Hicks, A. C., Jacob, R., Grieneisen, L. E., Brownlee, S. A., Muller, L. K., & Blehert, D. S. (2012). Frequent arousal from hibernation linked to severity of infection and mortality in bats with white-nose syndrome. *PLoS One*, *7*(6), e38920. https://doi.org/10.1371/journal.pone.0038920

Reichard, J. D., & Kunz, T. H. (2009). White-nose syndrome inflicts lasting injuries to the wings of little brown myotis (*Myotis lucifugus*). *Acta Chiropterologica*, *11*(2), 457–464. https://doi.org/10.3161/150811009x485684

Saeed, S., Bonnefond, A., Tamanini, F., Mirza, M. U., Manzoor, J., Janjua, Q. M., Din, S. M., Gaitan, J., Milochau, A., Durand, E., Vaillant, E., Haseeb, A., De Graeve, F., Rabearivelo, I., Sand, O., Queniat, G., Boutry, R., Schott, D. A., Ayesha, H., … Froguel, P. (2018). Loss-of-function mutations in ADCY3 cause monogenic severe obesity. *Nature Genetics*, *50*, 175–179. https://doi.org/10.1038/s41588-017-0023-6

Sahdo, B., Evans, A. L., Arnemo, J. M., Frobert, O., Sarndahl, E., & Blanc, S. (2013). Body temperature during hibernation is highly correlated with a decrease in circulating innate immune cells in the brown bear (*Ursus arctos*): A common feature among hibernators? *Internation Journal of Medical Sciences*, *10*(5), 508–514. https://doi.org/10.7150/ijms.4476

Schiebelhut, L. M., Puritz, J. B., & Dawson, M. N. (2018). Decimation by sea star wasting disease and rapid genetic change in a keystone species, *Pisaster ochraceus*. *Proceedings of the National Academy of Sciences*, *115*(27), 201800285. https://doi.org/10.1073/pnas.1800285115

Simmons, N. B., & Voss, R. S. (2009). Collection, preparation, and fixation of specimens and tissues. In T. H. Kunz & S. PArsons (Eds.), *Ecological and behavioral methods for the study of bats* (2nd ed., pp. 849–867). Baltimore, MD: The Johns Hopkins University Press.

Smit, A., Hubley, R., & Green, P. (2013–2015). RepeatMasker Open-4.0. Retrieved from http://www.repeatmasker.org

Spitzer, K., Pelizzola, M., & Fuschik, A. (2020). Modifying the chi-square and the CMH test for population genetic inference: Adapting to over-dispersion. *Annals of Applied Statistics*, *14*, 202–220.

Stergiakouli, E., Gaillard, R., Tavare, J. M., Balthasar, N., Loos, R. J., Taal, H. R., Evans, D. M., Rivadeneira, F., St Pourcain, B., Uitterlinden, A. G., Kemp, J. P., Hofman, A., Ring, S. M., Cole, T. J., Jaddoe, V. W., Davey Smith, G., & Timpson, N. J. (2014). Genome-wide association study of height-adjusted BMI in childhood identifies functional variant in ADCY3. *Obesity*, *22*(10), 2252–2259. https://doi.org/10.1002/oby.20840

Storey, K. B., & Storey, J. M. (2004). Mammalian hibernation: Biochemical adaptation and gene expression. In K. B. Storey (Ed.), *Functional metabolism: Regulation and adaptation*. John Wiley & Sons.

Tajima, F. (1989). The effect of change in population size on DNA polymorphism. *Genetics*, *123*, 597–601.

Therkildsen, N. O., & Palumbi, S. R. (2016). Practical low-coverage genomewide sequencing of hundreds of individually barcoded samples for population and evolutionary genomics in nonmodel species. *Molecular Ecology Resources*, *17*, 194–208. https://doi.org/10.1111/1755-0998.12593

Thompson, J. N. (1998). Rapid evolution as an ecological process. *Trends in Ecology & Evolution*, *13*(8), 329–332.

Vander Wal, E., Garant, D., Festa-Bianchet, M., & Pelletier, F. (2013). Evolutionary rescue in vertebrates: Evidence, applications and uncertainty. *Philosophical Transactions of the Royal Society of London. Series B, Biological Sciences*, *368*(1610), 20120090. https://doi.org/10.1098/rstb.2012.0090

Verant, M. L., Meteyer, C. U., Speakman, J. R., Cryan, P. M., Lorch, J. M., & Blehert, D. S. (2014). White-nose syndrome initiates a cascade of physiological disturbances in the hibernating bat host. *BMC Physiology*, *14*(10).

Vonhof, M. J., Russell, A. L., & Miller-Butterworth, C. M. (2015). Range-wide genetic analysis of little brown bat (*Myotis lucifugus*) populations: Estimating the risk of spread of white-nose syndrome. *PLoS One*, *10*(7), e0128713. https://doi.org/10.1371/journal.pone.0128713

Waples, R. K., Albrechtsen, A., & Moltke, I. (2019). Allele frequency-free inference of close familial relationships from genotypes or low-depth sequencing data. *Molecular Ecology*, *28*(1), 35–48. https://doi.org/10.1111/mec.14954

Waples, R. S., & Gaggiotti, O. (2006). What is a population? An empirical evaluation of some genetic methods for identifying the number of gene pools and their degree of connectivity. *Molecular Ecology*, *15*(6), 1419–1439. https://doi.org/10.1111/j.1365-294X.2006.02890.x

Waples, R. S., Luikart, G., Faulkner, J. R., & Tallmon, D. A. (2013). Simple life-history traits explain key effective population size ratios across diverse taxa. *Proceedings of the Royal Society B: Biological Sciences*, *280*(1768), 20131339. https://doi.org/10.1098/rspb.2013.1339

Weiner, J. A., & Jontes, J. D. (2013). Protocadherins, not prototypical: A complex tale of their interactions, expression, and functions. *Frontiers in Molecular Neuroscience*, *6*, 4. https://doi.org/10.3389/fnmol.2013.00004

Welinder, K. G., Hansen, R., Overgaard, M. T., Brohus, M., Sønderkær, M., von Bergen, M., Rolle-Kampczyk, U., Otto, W., Lindahl, T. L., Arinell, K., Evans, A. L., Swenson, J. E., Revsbech, I. G., & Frøbert, O. (2016). Biochemical foundations of health and energy conservation

in hibernating free-ranging subadult brown bear *Ursus arctos*. *Journal of Biological Chemistry*, *291*(43), 22509–22523. https://doi.org/10.1074/jbc.M116.742916

White, G. C., & Burnham, K. P. (1999). Program MARK: Survival estimation from populations of marked animals. *Bird Study*, *46*(Supplement), 120–138.

Wilder, A. P., Kunz, T. H., & Sorenson, M. D. (2015). Population genetic structure of a common host predicts the spread of white-nose syndrome, an emerging infectious disease in bats. *Molecular Ecology*, *24*(22), 5495–5506. https://doi.org/10.1111/mec.13396

Wright, S. (1930). Evolution in Mendelian populations. *Genetics*, *2*, 97–159.

Yeaman, S. (2015). Local adaptation by alleles of small effect. *American Naturalist*, *186*(Suppl. 1), S74–89. https://doi.org/10.1086/682405

SUPPORTING INFORMATION

Additional supporting information may be found online in the Supporting Information section.

How to cite this article: Gignoux-Wolfsohn SA, Pinsky ML, Kerwin K, et al. Genomic signatures of selection in bats surviving white-nose syndrome. *Mol Ecol*. 2021;00:1–15. https://doi.org/10.1111/mec.15813